

Numerical modeling of atmospheric circulation and pollution transport in the Norilsk valley

V.A. Shlychkov,¹ V.M. Malbakhov,² and A.A. Lezhenin²

¹*Novosibirsk Affiliate of the Institute of Water and Ecological Problems,
Siberian Branch of the Russian Academy of Sciences, Novosibirsk*

²*Institute of Computational Mathematics and Mathematical Geophysics,
Siberian Branch of the Russian Academy of Sciences, Novosibirsk*

Received December 17, 2004

Calculation results for local air circulation in the Norilsk valley are presented. Norilsk is located in the area with a complex topography with difference of level more than 1000 m. Orographical features in the city vicinity cause formation of mountain-and-valley circulation with a wide scatter of trajectories and a rapidly changing direction. To describe the air flow dynamics and pollutant redistribution, a numerical model of mesoscale atmospheric boundary layer was used. The model was adapted to the Norilsk natural-geographical conditions. The model estimates of sulphur dioxide fallout over the area are obtained for different meteorological situations.

Introduction

Administratively, Norilsk city is related to the Taimyr autonomous district. The city is located beyond the Polar circle near 69°N in the Norilsk valley of 170 km length and 40–60 km width oriented in the northwestern direction. On the south the valley is bounded by the Longdokoiskii Kamen' ridges of 600–700 m height; on the north and east – by the mountain system Putoran and some others with peaks of more than 1000 m.

The short cold summer stipulate a high sensitivity and low stability of natural complexes to ecological loads. Breakdown of the living soil cover presents a serious hazard for the tundra zone. Short vegetative period (60 days) limits the rate of biological cycle and determines low capacity of tundra ecosystems for regeneration. Reaching its tolerance limit, the wood vegetation in tundra, when destructing, can not be reconstructed. Besides, due to low temperatures and suppressed biological exchange, the resistivity of harmful substances increases and they are accumulated in natural systems.

The forest-tundra vegetation is very sensitive to atmospheric contaminants. The absorbing capability of northern forests relative to sulfur anhydride is no more than 16–18 kg per hectare that is tens times lower than in the forest zone of mid-latitudes. Some kinds of mosses and lichens of the Far North perish even at the sulfur anhydride concentration of 10% of the maximum permissible concentration in air. Along with the low ecological capacitance of nature, this raises the risk of ecological disasters.

On the territory of Norilsk the manufacturing plants of non-ferrous metallurgy – the State Metallurgical Integrated Plant (SMIP) Norilsk Nickel – are situated with the total volume of emissions more than 2 million tons per year,¹ and sulfur dioxide makes the most part of the emissions. The sulfur

anhydride and sulfates are the aggressive compounds, which refer to the priority ones. The industrial polluting of air basin, territories, and water objects by sulfur compounds leads to different unfavorable effects, including impairment of human health, degradation of forests, acidification of internal fresh-water basins.

Industrial emissions from SMIP affect the northern nature so strongly that disappearance and damage of vegetation are observed at distances more than 100 km from the source, and the impact zone increases with time.² In this connection, there is an urgent need for obtaining estimates of anthropogenic load on the adjacent territories and the contribution of the industrial zone to general pollution of the region. Apart from SO₂ emissions, of interest is a reliable determination of pollution flows across the boundaries of the region in the form of distant transport of greenhouse gases affecting climatic parameters of adjacent territories and the planet as a whole. This problem becomes urgent due to ratification of the Kyoto Protocol by the Russian Federation.

The Norilsk region is characterized by the rigorous climate and vast territory. In addition, the region is difficult to reach. All this sharply limits the possibility of performance of natural investigations. The modeling makes it possible to reproduce atmospheric processes for describing the transport and transformation of gas and aerosol impurities, as well as to obtain quantitative estimates of sulfate fallouts on the underlying surface.

Below we formulate the mathematical model of the mesoscale atmospheric boundary layer (ABL) to describe the local processes on a limited territory.³ The model is intended for calculation of the turbulent fields, wind, temperature, and humidity in the lower troposphere. As basic equations, we adopted the equations of atmospheric hydrothermodynamics written in the approximation of a deep convection.

The underlying surface is orographically and thermally inhomogeneous with natural-terrain and anthropogenic objects in the form of reservoirs, forests, bare soil, snow cover, urban conglomerates, industrial complexes, and so on.

Formulation of the problem

Let us introduce the Cartesian coordinates (x, y, z) , in which the axis x is directed to the east, y – to the north, and z – upward. Take a system of inelastic equations⁴ of hydrothermodynamics in the Boussinesq approximation as initial one. In thermodynamic fields, we separate out the basic (background) trend, reflecting the initial density of the atmospheric boundary layer (ABL)

$$\Theta = \bar{\Theta}(z) + \theta; T = \bar{T}(z) + T';$$

$$P = \bar{P}(z) + p; \Pi = \bar{\Pi}(z) + \pi, \quad (1)$$

where Θ , T , P , Π are the potential temperature, absolute temperature, pressure, and the Exner function (the pressure analog), respectively; the variables with a bar denote the background fields satisfying the equations of state and statics

$$\bar{P} = R_a \bar{\rho} \bar{T}; \quad \frac{d\bar{P}}{dz} = -\bar{\rho}g; \quad \bar{\Pi} = \frac{\bar{\Theta}}{\bar{T}}. \quad (2)$$

where $\bar{\rho}(z)$ is the static decrease of density with height; g is the acceleration of gravity, R_a is the gas constant of air. The Reynolds equations are considered to be initial, obtained as a result of averaging over a set of the Navier–Stokes equations⁵:

$$\begin{aligned} & \frac{\partial u}{\partial t} + u \frac{\partial u}{\partial x} + v \frac{\partial u}{\partial y} + \frac{1}{\bar{\rho}} w \frac{\partial \bar{\rho} u}{\partial z} = \\ & = -c_p \bar{\Pi} \frac{\partial \pi}{\partial x} + l v - \frac{1}{\bar{\rho}} \left(\frac{\partial \tau_{xx}}{\partial x} + \frac{\partial \tau_{xy}}{\partial y} + \frac{\partial \tau_{xz}}{\partial z} \right), \\ & \frac{\partial v}{\partial t} + u \frac{\partial v}{\partial x} + v \frac{\partial v}{\partial y} + \frac{1}{\bar{\rho}} w \frac{\partial \bar{\rho} v}{\partial z} = \\ & = -c_p \bar{\Pi} \frac{\partial \pi}{\partial y} - l u - \frac{1}{\bar{\rho}} \left(\frac{\partial \tau_{yx}}{\partial x} + \frac{\partial \tau_{yy}}{\partial y} + \frac{\partial \tau_{yz}}{\partial z} \right), \\ & \frac{\partial w}{\partial t} + u \frac{\partial w}{\partial x} + v \frac{\partial w}{\partial y} + \frac{1}{\bar{\rho}} w \frac{\partial \bar{\rho} w}{\partial z} = \\ & = -c_p \bar{\Pi} \frac{\partial \pi}{\partial z} + \lambda \vartheta + 0.61 g q - \frac{1}{\bar{\rho}} \left(\frac{\partial \tau_{zx}}{\partial x} + \frac{\partial \tau_{zy}}{\partial y} + \frac{\partial \tau_{zz}}{\partial z} \right), \\ & \frac{\partial \vartheta}{\partial t} + u \frac{\partial \vartheta}{\partial x} + v \frac{\partial \vartheta}{\partial y} + \frac{1}{\bar{\rho}} w \frac{\partial \bar{\rho} \vartheta}{\partial z} + S w = \\ & = -\frac{1}{\bar{\rho}} \left(\frac{\partial \sigma_x}{\partial x} + \frac{\partial \sigma_y}{\partial y} + \frac{\partial \sigma_z}{\partial z} \right) - \frac{1}{\bar{\rho} c_p} \frac{\partial R}{\partial z} + \Phi_T, \\ & \frac{\partial \bar{\rho} u}{\partial x} + \frac{\partial \bar{\rho} v}{\partial y} + \frac{\partial \bar{\rho} w}{\partial z} = 0, \end{aligned} \quad (3)$$

where ϑ denotes the disturbances of potential temperature, q is the specific humidity, l is the Coriolis parameter, λ is the parameter of buoyancy, c_p is the air specific heat, $S = \partial \bar{\Theta} / \partial z$ is the temperature stratification, R is the radiation flux, Φ_T denotes the phase heat fluxes, τ_{ij} denotes the components of tensor of turbulent stresses. The set of equations (3) is taken as basic when constructing the ABL mesoscale model.

The relationships of turbulent closure are formulated under the assumption that horizontal and vertical processes are anisotropic. To describe the horizontal diffusion, the Smagorinsky model is used, and the vertical vortex viscosity is calculated using two-parametric model of semiempirical theory of turbulence. The turbulence model in terms of τ_{ij} has the form⁶:

$$\begin{aligned} \tau_{xx} &= K_s D_T, \quad \tau_{yy} = -K_s D_T, \quad \tau_{xy} = \tau_{yx} = K_s D_S, \\ \tau_{zx} &= K_s w_x, \quad \tau_{zy} = K_s w_y, \quad \tau_{xz} = K_z u_z, \\ \tau_{yz} &= K_z v_z, \quad \tau_{zz} = K_z w_z, \end{aligned} \quad (4)$$

where

$$D_T = u_x - v_y, \quad D_S = v_x + u_y$$

are the components of plane strain, and the coefficient of horizontal turbulent exchange is calculated using the Smagorinsky relation

$$K_s = \alpha \Delta s \sqrt{D_T^2 + D_S^2};$$

where $\Delta s = \Delta x \cdot \Delta y$ is the area of an elementary x, y -cell, α is the proportionality factor. To describe the vertical turbulent exchange, the evolution equations for kinetic turbulence energy b and its dissipation rate ε are used⁷:

$$\begin{aligned} & \frac{\partial b}{\partial t} + u \frac{\partial b}{\partial x} + v \frac{\partial b}{\partial y} + \frac{1}{\bar{\rho}} w \frac{\partial \bar{\rho} b}{\partial z} = \\ & = \frac{\partial}{\partial x} K_s \frac{\partial b}{\partial x} + \frac{\partial}{\partial y} K_s \frac{\partial b}{\partial y} + \frac{\partial}{\partial z} K_z \frac{\partial b}{\partial z} + J_1 - \varepsilon, \\ & \frac{\partial \varepsilon}{\partial t} + u \frac{\partial \varepsilon}{\partial x} + v \frac{\partial \varepsilon}{\partial y} + \frac{1}{\bar{\rho}} w \frac{\partial \bar{\rho} \varepsilon}{\partial z} = \\ & = \frac{\partial}{\partial x} K_s \frac{\partial \varepsilon}{\partial x} + \frac{\partial}{\partial y} K_s \frac{\partial \varepsilon}{\partial y} + \frac{\partial}{\partial z} K_z \frac{\partial \varepsilon}{\partial z} + c_2 \frac{\varepsilon}{b} J_1 - c_3 \frac{\varepsilon^2}{b}, \\ & K_z = c_1 \frac{b^2}{\varepsilon}, \end{aligned}$$

where

$$J_1 = \frac{1}{2} K_z (u_z^2 + v_z^2 + w_z^2) - \alpha_\theta K_z \lambda \bar{\Theta}_z$$

is the source supplementing the turbulence energy, c_1, c_2, c_3 are the universal constants.

Let us determine the domain of solution in the form of rectangular parallelepiped with uneven bottom boundary reflecting the inhomogeneity of the underlying surface relief:

$$0 \leq x \leq L_x, \quad 0 \leq y \leq L_y, \quad \delta \leq z \leq H, \quad (5)$$

where L_x , L_y are the horizontal dimensions of the domain, the function $z = \delta(x, y)$ sets the relief, H is the position of the upper boundary. A limitation on the horizontal scales of reproducible phenomena is related to neglect of the Earth's surface sphericity in the initial equations and the neglect of β -effect (change of the Coriolis parameter along meridian). The cited effects can be considered unessential at the domain dimensions not exceeding 1000 km.

Let us formulate the basic set of boundary conditions for the system (3) in the form:

$$\begin{aligned} \frac{\partial u}{\partial x} = \frac{\partial v}{\partial x} = \frac{\partial w}{\partial x} = 0, \quad \frac{\partial \vartheta}{\partial x} = 0 \quad \text{at } x = 0, \quad x = L_x; \\ \frac{\partial u}{\partial y} = \frac{\partial v}{\partial y} = \frac{\partial w}{\partial y} = 0, \quad \frac{\partial \vartheta}{\partial y} = 0 \quad \text{at } y = 0, \quad y = L_y. \end{aligned} \quad (6)$$

In the bottom part of the ABL immediately at the underlying surface we separate out the layer of constant fluxes (CFL) of the thickness h , in which the vertical gradients of the fields far exceed their values in the upper layers. In the numerical models of ABL the parametrization is commonly used, based on the Monin–Obukhov similarity theory.⁸ Write the basic relations of the similarity theory, which serve boundary conditions at the bottom boundary of the region

$$\begin{aligned} K_z \frac{\partial u}{\partial z} = c_u |\mathbf{u}| u, \quad K_z \frac{\partial v}{\partial z} = c_u |\mathbf{u}| v; \quad w_n = 0; \\ K_z \frac{\partial \Theta}{\partial z} = c_T |\mathbf{u}| (\theta - \theta_0) \quad \text{at } z = h + \delta, \end{aligned} \quad (7)$$

where c_u , c_T are the coefficients of resistance and heat exchange, calculated using the model of CFL, θ_0 is the temperature of underlying surface, w_n is the velocity component normal to the Earth's surface.

For the upper boundary we lay down the condition of the form

$$u = \mathbf{U}, \quad v = \mathbf{V}, \quad p = p_H, \quad \frac{\partial \theta}{\partial z} = S_0 \quad \text{at } z = H, \quad (8)$$

where \mathbf{U} , \mathbf{V} are vectors of the external (large-scale) wind velocity in the free atmosphere, p_H is the specified baric field, S_0 is the static stability of the standard atmosphere.

As initial conditions, we take the horizontally homogeneous stationary solution of the problem at the stable stratification of ABL.

Transfer model and impurity diffusion

Equations of the semiempirical theory of diffusion and impurity transfer in ABL are of the form⁶:

$$\begin{aligned} \frac{\partial \mathbf{C}}{\partial t} + u \frac{\partial \mathbf{C}}{\partial x} + v \frac{\partial \mathbf{C}}{\partial y} + \frac{1}{\bar{\rho}} w \frac{\partial \bar{\rho} \mathbf{C}}{\partial z} - \frac{w_g}{\bar{\rho}} \frac{\partial \bar{\rho} \mathbf{C}}{\partial z} = \\ = \frac{1}{\bar{\rho}} \left(\frac{\partial}{\partial x} \bar{\rho} K_x \frac{\partial \mathbf{C}}{\partial x} + \frac{\partial}{\partial y} \bar{\rho} K_y \frac{\partial \mathbf{C}}{\partial y} + \frac{\partial}{\partial z} \bar{\rho} K_z \frac{\partial \mathbf{C}}{\partial z} \right) + \\ + I_{\mathbf{C}} + \mathbf{F}(\mathbf{C}), \end{aligned} \quad (9)$$

where $\mathbf{C}(x, y, z, t)$ is the vector of impurity concentration; $I_{\mathbf{C}}$ is the emission power; w_g is the sedimentation rate; $\mathbf{F}(\mathbf{C})$ is the matrix of chemical transformation of impurity components.

The boundary conditions at the bottom boundary are

$$K_z \frac{\partial \mathbf{C}}{\partial z} = \gamma \mathbf{C} \quad \text{at } z = h + \delta, \quad (10)$$

where γ is the rate of dry (surface) deposition.

At the upper boundary, the following condition is given:

$$K_z \frac{\partial \mathbf{C}}{\partial z} = 0 \quad \text{at } z = H. \quad (11)$$

During transportation, SO_2 is chemically transformed into sulfates and sulfuric acid, which, as a result of washing out by precipitation, fall out on the underlying surface as acid rains. In our case we consider a two-component impurity $\mathbf{C} = (C_1, C_2)$ containing the primary substance $C_1 = \text{SO}_2$ and sulfates $C_2 = \text{SO}_4^{2-}$.

The following transformations of the impurities are taken into account in the model. Emitted of sulfur dioxide in the process of spatial redistribution, at the cost of advection, diffusion, and vertical mixing, is partly absorbed by underlying surface, partly falls out with precipitation and also turns into sulfate-ions. These sulfates along with the transfer and diffusion are subjected to dry and moist precipitation. When considering the system of chemical transformations as an isolated stage of the splitting method, we write it in the component form⁹

$$\frac{\partial C_1}{\partial t} = -k_1 C_1 - n_1 C_1, \quad \frac{\partial C_2}{\partial t} = \beta k_1 C_1 - n_2 C_2, \quad (12)$$

where k_1 is the rate of chemical transformation of SO_2 in sulfates, n_1 , n_2 are rates of C_1 , C_2 washing out by precipitation, β is the relation between molecular masses of SO_4^{2-} and SO_2 . The model (12) was approved in the problems of transfer of sulfur compounds.¹⁰

Insert the curvilinear coordinate system,⁷ in which the surface $z = \delta(x, y)$ is the coordinate plane

$$x' = x; \quad y' = y; \quad z' = \frac{z - \delta}{1 - \delta/H}. \quad (13)$$

Transformed according to Eq. (13), Eqs. (3) were solved by the method of final differences³ with respect to variables x' , y' , z' , t . To integrate with respect to time, we used the implicit predictor–corrector¹¹ splitting method, modified in order to increase the norm of the transition operator and to raise the algorithm stability. When solving the boundary problem for vertical direction, the iterations by orographic components were used.

Calculation of wind regime

The formulated model is used for reproducing the spatial structure of the air flow in the Norilsk region at a given flow in the free atmosphere.

Consider the area of $400 \times 400 \text{ km}^2$ dimension and set the upper boundary of the calculated parallelepiped $H = 3000 \text{ m}$. The discretization of equations can be made on the uniform grid containing $128 \times 128 \times 90$ nodes and a time step of 90 s.

We locate the origin of the Cartesian rectangular coordinate system at a point with geographical coordinates 67.5°N and 83.2°E , so that the region center coincided with the center of Norilsk, and the origin was in the left bottom angle of the region.

As initial conditions, we set the stable temperature stratification with a standard gradient $S_0 = 0.003^\circ\text{C}/\text{m}$ and obtain the wind field at $t = 0$ from the stationary solution of a horizontally homogeneous problem.

The multilayer digital topographic map SRTM-30 with the 30 s resolution (925 m) was chosen from NASA web site and interpolated to the our grid by means of GIS.

Taking into account the predominant west-eastern direction of transfer in the free atmosphere, we set the speed of zonal flow as $U = 10 \text{ m/s}$, $V = 0$. These parameters determine the right parts of boundary conditions (8). The problem was solved for determination of the spatial distribution of wind velocity due to orographic forcing. The daily variation of meteorological parameters was not taken into account.

Vertical distribution of velocity model components u and v at the point $x = 92 \text{ km}$, $y = 3 \text{ km}$ (corresponding to location of Igarka city) was compared with the available statistical mean profiles of wind velocity from aerological data of Igarka meteorological station. A qualitative agreement of velocity fields was detected, namely, formation of the ground opposite flow ($u < 0$) in the lower layers at $z < 300 \text{ m}$; the clockwise wind shift with height in the middle part of ABL; and the west-eastern transfer to the level $z = 3 \text{ km}$.

The model wind velocity in Norilsk has a complicated vertical structure (Fig. 1). In the near ground layer the wind is directed from the north-west along the Norilsk hollow. Above, the velocity vector experiences rotation, so that in the layer $1000 < z < 1500$, a facing flow is formed, caused by the flow around the Putoran plateau. At a higher altitude ($z \approx 1600 \text{ m}$), a stagnation zone is located where the velocity modulus tends to zero. On approaching the top boundary of the region, the summarized angle of the velocity rotation exceeds 360° .

As a whole, the western flow undergoes stagnation due to influence of high mountain ridges in the east of the region. A complex wind structure is shown by the profile w variable with height (dashed line in Fig. 1), constructed by the maximum value of 8 cm/s .

For analysis of velocity fields, we calculated trajectories in the horizontal plane at different levels. In the atmospheric boundary layer, the particles move mainly in the south-eastern direction, which corresponds to the Norilsk valley orientation. The valley with high edges forms some kind of canyon, which makes the western flow to turn south and move along the slopes.

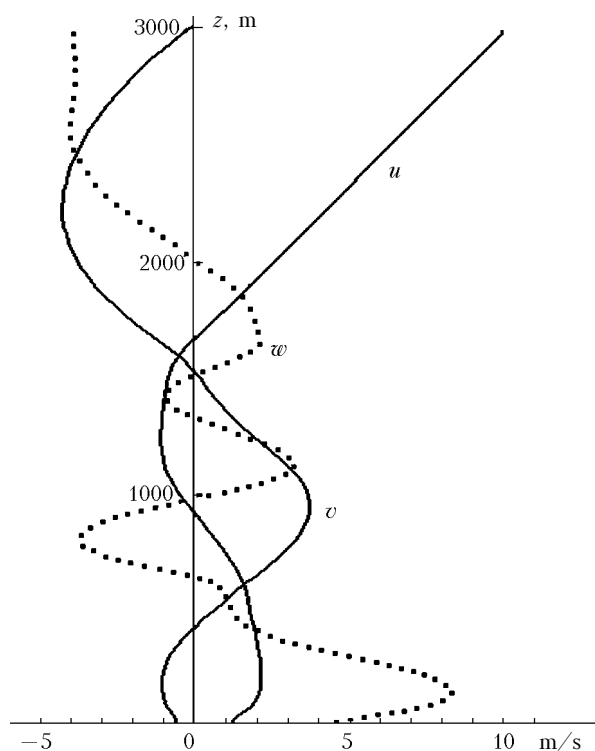


Fig. 1. Calculated profiles of zonal (u) and meridional (v) components of wind velocity in Norilsk. The distribution of vertical velocity w is denoted by a dashed curve.

At a height of 1000 m, a comparatively light north-eastern wind is grown up and the particles are shifted facing the basic flow. Close to the upper boundary ($z = 2000 \text{ m}$), the wind shift occurs due to the Coriolis forces. The south-western wind becomes predominant in the flow structure. The effect of its going round high eastern ridges evidently manifests itself. Individual particles, arriving at zones of divergence or convergence, move away to great distance from the initial level and can change the direction of movement.

In conclusion it should be noted that the topographic peculiarities in the Norilsk region play a decisive role when forming stationary or slowly varying flows. The wind field has an inhomogeneous horizontal structure and significantly varies with height. At different levels, the advection directions significantly differ, including opposite flows and closed rotations.

Calculation of concentration field and SO_2 fallouts

The calculated wind velocity and turbulence fields were used to estimate the pollution of the territory and air basin by the SO_2 emissions from SMIP Norilsk Nickel. The total volume of SO_2 emissions is arbitrarily taken to be 2 million tons per year, which makes about 63.5 kg/s . Integration of Eqs. (9) is

carried out up to establishment of stationary regime, at which the spatial structure of the concentration field does not vary with time.

Keeping in mind a preliminary character of calculations and taking into account that at comparatively short distances from the source the chemical transformation of SO_2 is not important, we have restricted ourselves to the case of a passive transfer of one-component contamination, assuming in Eq. (12) $C_2 = 0$, $k_1 = 0$.

In accordance with Eq. (12), there can be two mechanisms for contaminations to leave the atmosphere: dry deposition on the underlying surface, taken into account as the boundary condition (10), and washing-out by precipitations. The calculations have shown that at time scales of the order of one day and at distances of tens of kilometers, the second mechanism is dominant. In this case, sensitivity of the model to variations of n_1 (rate of washing-out) is much higher than to γ_1 (dry deposition).

The value of n_1 equal to 10^{-4} s^{-1} (Ref. 9), is oriented to be used in the model MCTS-B for describing the transboundary transport of sulfur compounds over territories with characteristic scales of 1 000 km. This n_1 is based on the average-statistical structure of large-scale precipitation and in the framework of mesoscale modeling gives strongly overestimated

volumes of precipitation in the source vicinity. In this connection, we conduct the parametrization of the wet precipitation by a more physically substantiated method using the sedimentation mechanism. Let us set in Eq. (9) $w_g = 10^{-3} \text{ m/s}$, i.e., the fallout rate of contaminations, carried away by precipitation. For dry deposition we use the recommended⁹ $\gamma_1 = 0.012 \text{ m/s}$.

Figure 2 shows isolines of SO_2 concentration in the atmospheric boundary layer. The concentration maximum turns out to be shifted south-east roughly by 60 km, and the extreme values exceed 1 mg/m^3 at a standard daily mean maximum permissible concentration of 0.05 mg/m^3 . Note that the concentration field configuration varies with altitude. Thus, at $z = 900 \text{ m}$ the contamination plume is extended to the north along the mean wind direction at this height.

When leaving the atmosphere, SO_2 drops out on the underlying surface. The rate of impurity accumulation on the ground is shown in Fig. 3. The maximum precipitation is observed at a distance of 40–60 km from the center of emission. According to the spaceborne data,² just in this region the large-scale destruction of larch was noted. As a whole, the territory shown in the figure is close to location of the destroyed forest area.²

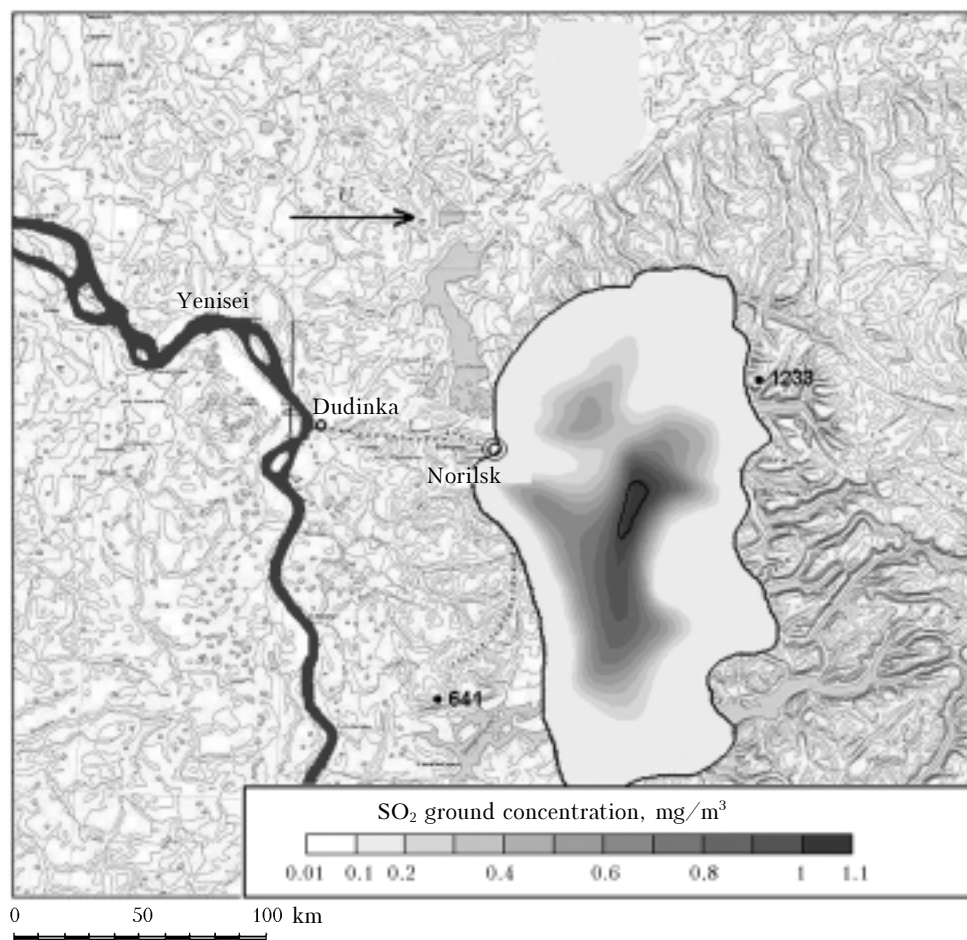


Fig. 2. Isolines of SO_2 ground concentration field.

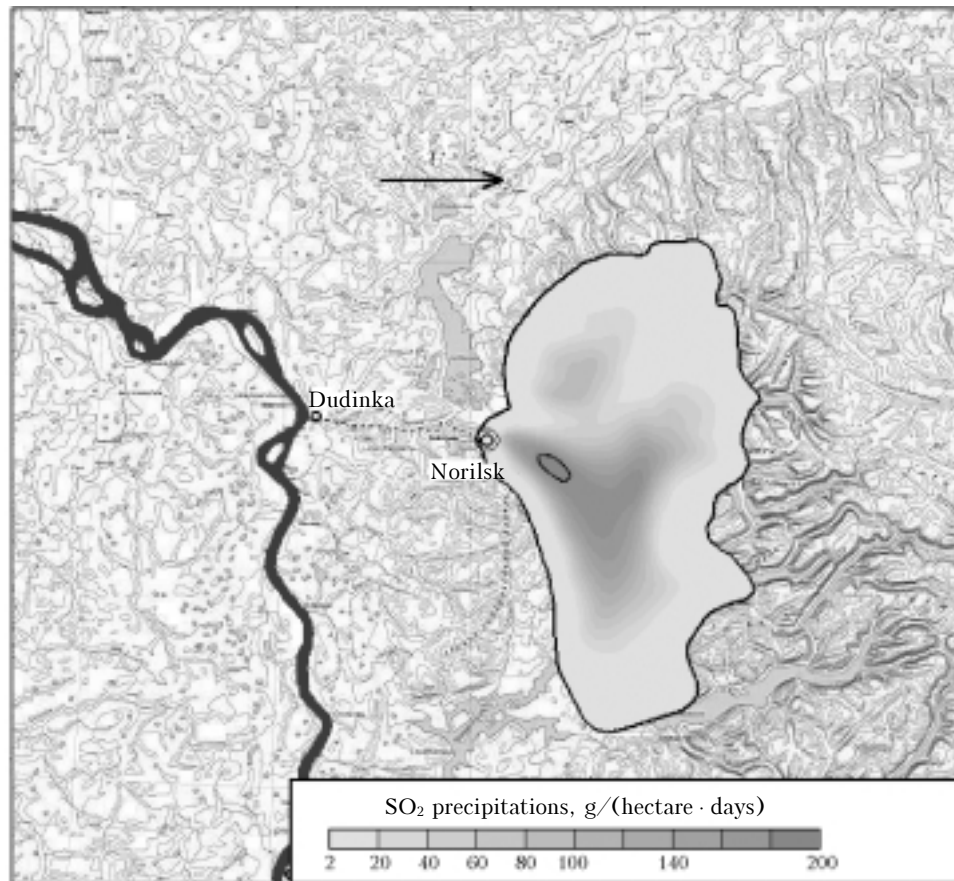


Fig. 3. Isolines of SO₂ precipitation field.

Conclusion

The paper describes the mathematical model of mesoscale atmospheric boundary layer capable to reconstruct turbulent flows under complicated physical-geographic conditions. The model is based on the equations of hydrothermodynamics written in the approximation of deep convection, that allows one to describe wave processes of the orographic nature in the lower and middle troposphere.

It would be prematurely to give real estimates of the Norilsk region pollution based on the performed investigation, because a lack of representative data base did not allow us to make a rigorous calibration of the model's inner parameters. Nevertheless, the presented preliminary results allow us to say that the mesoscale model of ABL, more or less identically reproduces main characteristics of local atmospheric circulation and peculiarities of pollutant transport under conditions of the Norilsk valley.

Acknowledgments

This work is supported by the Russian Foundation for Basic Research (grant No. 03–05–65279).

References

1. E.Yu. Bezuglaya, G.P. Rastorgueva, and I.V. Smirnova, *Breath of Industrial City* (Gidrometeoizdat, Leningrad, 1991), 255 pp.
2. V.I. Kharuk, K. Vinterberger, G.M. Tsibulski, and A.P. Yakhimovich, *Issled. Zemli iz Kosmosa*, No. 4, 91–97 (1995).
3. V.A. Shlychkov, *Aerosols of Siberia* (SB RAS Publishing House, Novosibirsk, 2005), 612 pp.
4. N.S. Veltishchev and A.A. Zhelmin, *Tr. Gidromettsentra SSSR*, Is. 238, 36–48 (1981).
5. *Atmospheric Turbulence and Modeling of Impurity Propagation* (Gidrometeoizdat, Leningrad, 1985), 351 pp.
6. V.V. Penenko and A.E. Aloyan, *Models and Methods for Problems of Environmental Protection* (Nauka, Novosibirsk, 1985), 256 pp.
7. B.B. Ilyushin and A.F. Kurbatskii, *Izv. Ros. Akad. Nauk, Ser. Fiz. Atmos. Okeana*, **30**, No. 5, 615–622 (1994).
8. A.S. Monin and A.M. Yaglom, *Statistical Hydrodynamics* (Gidrometeoizdat, St. Petersburg, 1992), Vol. 1, 694 p.
9. *Model Estimates of Sulfur Compound Precipitation Close to Pollution Sources and at Subgrid Level (Subregion of St. Petersburg)* (EMER/MSTS-B report 9/95, Moscow, 1995), 52 pp.
10. V.A. Shlychkov, *Atmos. Oceanic Opt.* **11**, No. 6, 517–520 (1998).
11. G.I. Marchuk, *Methods of Computational Mathematics* (Nauka, Novosibirsk, 1973), 352 pp.